Available online at www.sciencedirect.com
SCIENCE DIRECT®
ELSEVIER
Journal of Magnetism and Magnetic Materials 257 (2003) 32–43
journal of magnetism and magnetic materials
www.elsevier.com/locate/jmmm

Mechanical properties of Nylon bonded Nd–Fe–B permanent magnets

Monika G. Garrell[a], Albert J. Shih[b,*], Bao-Min Ma[c], Edgar Lara-Curzio[d], Ronald O. Scattergood[e]

[a] *Department of Mechanical and Aerospace Engineering, NC State University, Raleigh, NC 27695, USA*
[b] *Department of Mechanical Engineering, University of Michigan, Ann Arbor, MI 48109, USA*
[c] *Magnequench Technical Center, Research Triangle Park, NC 27709, USA*
[d] *High Temperature Materials Laboratory, Oak Ridge National Laboratory, Oak Ridge, TN 37831, USA*
[e] *Department of Materials Science and Engineering, NC State University, Raleigh, NC 27695, USA*

Received 16 April 2002; received in revised form 8 August 2002

Abstract

Tensile and flexural strengths as well as Young's modulus of Polyamide-11 (Nylon-11) based injection molded Nd–Fe–B magnets have been determined from −40°C to 100°C. Two types of Nd–Fe–B powders were included in this study. One is the conventional melt spun powder of irregular shape, the other is the atomized powder of spherical morphology. It was found that the tensile strength varies significantly with both test temperature and morphology of Nd–Fe–B powder. For a fixed volume fraction of magnet powder, the tensile strength decreases with increasing temperature. For bonded magnets made of melt spun powder, the tensile strength increases with increasing volume fraction of magnet powder. Specimens made of spherical atomized powders exhibit much lower tensile strength and better flexibility when compared to those made of melt spun powder. Scanning electron microscopy (SEM) analysis indicated that the debonding at the Nd–Fe–B powder and Nylon interface is the main cause of failure at 23°C and 100°C. At −40°C, a different failure mechanism with the fracture of Nd–Fe–B particle was observed on magnets prepared from melt spun powders. For the specimen containing 59.7 vol% of melt spun powder, a bending strength of 41 MPa and dynamic Young's modulus of 12.7 GPa were obtained.

Keywords: Bonded magnets; Melt spun NdFeB; Atomized NdFeB; Mechanical properties

1. Introduction

Since the introduction of $Nd_2Fe_{14}B$-based magnets in the 1980s [1,2], much research has been conducted to improve their intrinsic properties and to develop cost-efficient fabrication techniques. Injection molding has been found to produce isotropic bonded magnets with near net-shape. It can also be used as an effective way for low-cost, high-volume production of high performance magnets with complicated geometry.

Polyamide (Nylon) and polyphenylene-sulfide (PPS) are commonly used as polymer binders for injection molding of Nd–Fe–B-type magnets.

*Corresponding author. Tel.: +1-7346471766; fax: +1-7349360363.
E-mail address: shiha@umich.edu (A.J. Shih).

0304-8853/03/$ - see front matter
PII: S0304-8853(02)00983-6

Nylon has been known for many decades and its basic characteristics as well as processing parameters have been established. This enables Nylon to be used as polymer binder for injection molded magnets. The magnetic properties of bonded magnets have been previously studied and reviewed by many investigators [3,4]. In addition to the magnetic properties, mechanical properties of bonded magnets also play critical roles for many advanced applications. However, the temperature-dependent mechanical strengths of bonded magnets are not readily available in open literature for magnet designers. Previously, bending strength, fracture toughness and uniaxial tensile strength of sintered Nd–Fe–B magnets have been reported [5–7]. Ikuma et al. [8] measured the shear strength of extrusion-molded Nd–Fe–B magnets. Xiao and Otaigbe [9] studied the effect of liquid crystal polymer and surface modification on mechanical properties of PPS bonded magnets. Tensile and bending strengths of PPS bonded magnets have also been reported [10].

The objective of this study was to determine the mechanical properties, namely tensile strength, bending strength, and Young's modulus, of Nylon-11 bonded Nd–Fe–B magnets at cryogenic, ambient, and elevated temperatures.

2. Experimental procedure

Two types of Nd–Fe–B powders were included for this study. One is the melt spun powder of irregular plate shape, as shown in Fig. 1(a). The other is the spherical powder, as shown in Fig. 1(b), prepared by inert gas atomization. The melt spun powders are flakes about 10–400 μm in size. The diameter of atomized powders ranges from 5 to 90 μm with the average around 50 μm.

These powders were mixed with Nylon-11 resin, lubricants, and other additives according to the predetermined mixing ratios for achieving the targeted volume fractions of magnetic powder in finished magnets. These mixtures were blended, compounded in a twin screw extruder, and pelletized into cylindrical pieces of about 5 mm in diameter and 3 mm in thickness. These pelletized compounds were dried to a dew point of −40°C to assure moisture removal before injection molding. They were then injection molded to obtain test specimens defined by the ASTM standards [11–13].

Test procedures were conducted according to the ASTM standards D638-99 [11], D790-99 [12] and C1259-98 [13] for tensile strength, flexural bending strength, and dynamic Young's modulus measurement, respectively. Tensile strength was tested at −40°C, 23°C, and 100°C. Bending tests and dynamic Young's modulus measurements were performed at 23°C. Scanning electron microscopy (SEM) was used to examine the fracture surface of test pieces to gain the insight into potential failure mechanisms.

2.1. Machine setup for tensile tests

The standard type-IV specimen specified in ASTM Standard D638-99 was injection molded. This dog-bone shaped specimen has a rectangular cross-section, 3.2 mm thick and 6 mm wide. The total length of the specimen is 115 mm. The gauge length of the test section was 60.08 mm as determined by a stress analysis using the finite-element method [14].

Tensile tests were performed on a MTS 808 machine. TestWare software was used for data acquisition and machine control. A 1000 N load cell was used to measure the force applied to the specimen. The engineering stress was determined by dividing the force applied by the original cross-sectional area. For tensile tests at room temperature, the engineering strain was calculated based on the extensometer data. For bonded magnets with spherical shape powder under light load (less than 30 N) and large strain, the engineering strain was estimated by dividing the cross-head displacement with the calculated gauge length.

Tensile tests were conducted at −40°C, 23°C and 100°C. For 23°C tensile tests, specimens were conditioned under a 50% relative humidity (50% RH) by leaving them in the test chamber for 48 h. The cross-head speed for these tests was 0.02 mm/s.

An applied test systems (ATS) furnace was used in conjunction with an ATS PID-controller, as shown in Fig. 2(a), for the −40°C and 100°C tests.

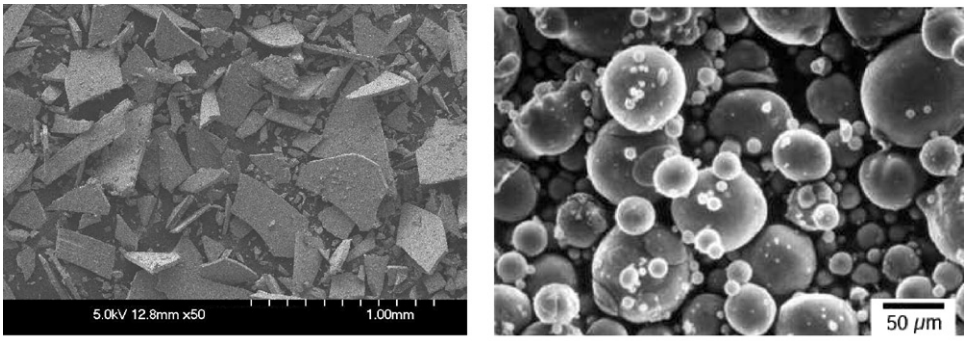

(a) (b)

Fig. 1. SEM micrographs of the two types of Nd–Fe–B powders used in this study (a) irregular, plate shape powder made by melt spinning and grinding and (b) spherical shape powder made by atomization.

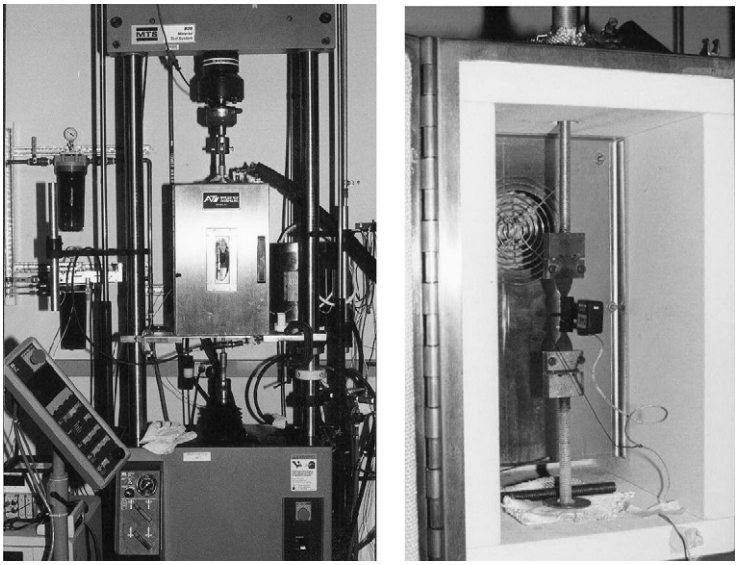

(a) (b)

Fig. 2. Setup of the cryogenic and elevated temperature tensile tests: (a) overview of the testing machine and (b) sample and grip inside the furnace.

Fig. 2(b) shows the sample and grips inside the furnace. A type-K thermocouple was mounted to the specimen to monitor test temperature and was also used to assure that the specimens reached the desired temperatures. For elevated temperature tensile tests, the ATS controller was set at 113°C and the specimens were soaked for 20 min after initializing the heating process to ascertain the desired temperature distribution throughout the specimen before initializing the test. For cryogenic tensile tests, the ATS furnace was connected to a liquid nitrogen tank. The controller was set at −42°C. The samples were soaked for 10 min to assure a uniform temperature distribution of −40°C throughout the specimen. The cross-head speed for the cryogenic tests was set to 0.01 mm/s.

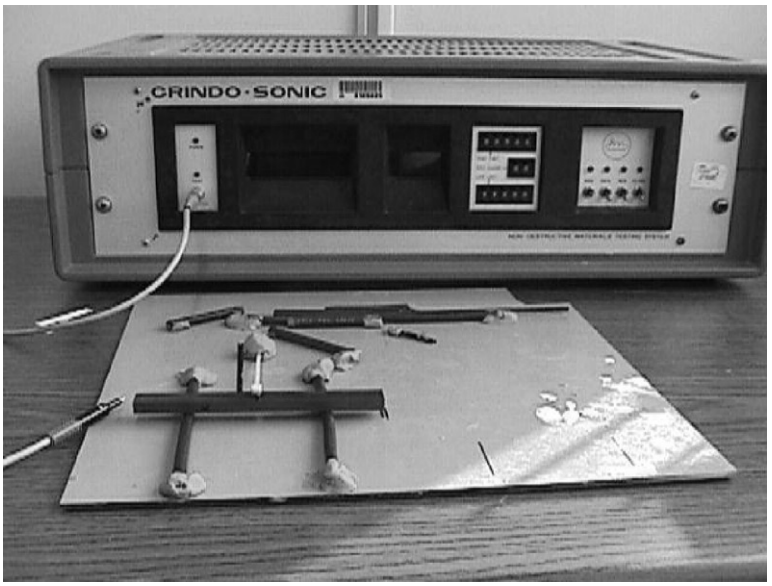

Fig. 3. Specimen, impulser, testing machine, and setup for dynamic Young's modulus measurement.

2.2. Machine setup for flexural tests

The four-point flexural bending tests were performed on a MTS 120 testing machine. The span between the supporting rollers is twice the span of the loading rollers, namely 76.2 and 38.1 mm, respectively. During the flexural bending test, a fixture guides the position of the loading rollers to maintain the same distance to the supporting rollers. The cross-head speed was set to 0.02 mm/s. The specimen dimensions were 125.7 mm × 6.4 mm × 12.7 mm. Only room temperature tests at 23°C and 50% RH were conducted.

2.3. Ultrasonic measurement of Young's modulus

The dynamic Young's modulus was measured according to the ASTM Standard C1259-98 [13] in conjunction with a GRINDO-SONIC MK4i instrument. The nominal specimen dimensions were 127.1 mm × 6.4 mm × 12.7 mm. This geometry enabled the measurement of the out-of-plane-flexure vibration of the beam. Fig. 3 shows the specimen, the ultrasonic testing machine, transducer, test specimen, and impulser used in this study. The fundamental resonant frequency of a free–free beam, i.e., assuming no external support on the beam during vibration, and its geometry were used to calculate the dynamic Young's modulus.

2.4. Specimen designation

Table 1 summarizes the sample designation, volume fraction, and powder type of Polyamide-11 based Nd–Fe–B specimens used in this study. Specimens of Ny597 and Ny710 were prepared from melt spun powder with volume fraction of 59.7% and 71.0%, respectively. Specimens of NyZK620 were prepared from atomized powder with a volume fraction of 62%. Tensile tests were also performed on pure Nylon specimens without any additives and are denoted by Ny.

3. Results and discussion

3.1. Tensile strengths

Five tensile tests each were carried out on Ny597, Ny710, Ny, and NyZK620 at −40°C, 23°C, and 100°C. Fig. 4 shows the engineering

Table 1
Sample designation and volume fraction of three samples used in this study

Numbering scheme	Estimated volume percent of Nd–Fe–B (%)	Magnetic powder type
Ny597	59.7	Irregular plate shape, melt spun
Ny710	71.0	Irregular plate shape, melt spun
NyZK620	62.0	Spherical shape, atomized
Ny	0	None

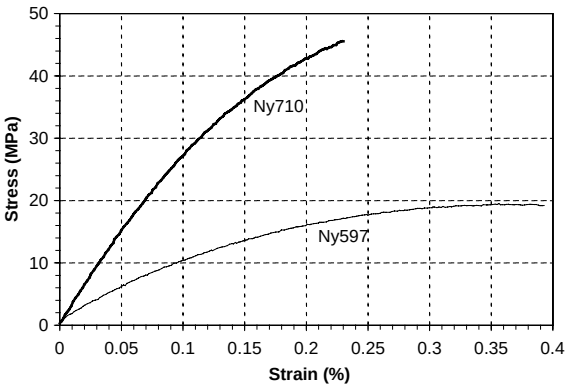

Fig. 4. Tensile stress–strain curves of Ny597 and Ny710 at 23°C.

stress–strain curves of Ny597 and Ny710 measured at 23°C. Each curve represents the arithmetic average of five tests from each testing group. The standard deviation for these tensile strengths is less than 4.1 MPa, indicating that the samples were of uniform quality and the tests were reproducible. Because of the higher volume fraction of magnetic powder, the Ny710 exhibits a higher tensile strength (47.8 vs. 18.4 MPa) and lower strain-to-fracture (0.23% vs. 0.39%) than that of Ny597. The difference in tensile strength and strain-to-fracture of these two samples indicates that characteristics of the morphology and the volume fraction of melt spun Nd–Fe–B powders contribute significantly to the overall tensile properties of Nylon bonded specimens.

Fig. 5 compares the ultimate tensile strength, S_{ut}, of Ny597, Ny710, Ny, and NyZK620 at −40°C, 23°C and 100°C. In general, S_{ut} decreases with increasing temperature with the exception of Ny710 at −40°C and 23°C. The S_{ut} values of Ny710 at −40°C and 23°C are of approximately the same magnitude. Moreover, Ny710 shows higher S_{ut} than that of Ny597 at all three test temperatures, suggesting that S_{ut} increases with increasing volume fraction. At 100°C, drastic reduction in S_{ut} was observed for Ny597, Ny710, and Ny. The S_{ut} values of NyZK620 with spherical shape powder are significantly lower than those of Ny597 or Ny710. At −40°C and 23°C, the S_{ut} values of NyZK620 are 8.3 and 4.8 MPa, respectively. These values are about 40% of those of Ny597. This decrease in S_{ut} may be attributed to the weak retention of spherical particles in the Nylon matrix. At 100°C, the S_{ut} of NyZK620 increases slightly. This requires further research for explanation.

Fig. 6 shows the stress vs. cross-head displacement curves of NyZK620 at −40°C, 23°C, 80°C, and 100°C. Due to the difficulty to get repetitive reading from extensometer for tensile tests at cryogenic and elevated temperature, the strain in Fig. 6 is calculated using the cross-head displacement divided by the 60.08 mm gauge length without the compensation for machine compliance. The relatively low load (less than 30 N) and large deformation make the error due to machine compliance less significant in testing the NyZK620 specimens. Two distinct types of stress–displacement curves can be noticed for data taken at −40°C and 23°C and 80°C and 100°C. These differences in stress–displacement behavior can be explained by the glass transition of the Nylon-11 at a temperature, T_g, of about 50°C [15]. For test temperatures below T_g, namely, −40°C and 23°C, the Nylon matrix is crystalline and deforms rigidly, while at temperatures above T_g, namely, 80°C and 100°C, Nylon matrix becomes partially amorphous. The amorphous regions deform thermoplastically while the crystalline regions deform as a rigid solid [16]. The apparent strain hardening effect is due in part to the increased flow resistance

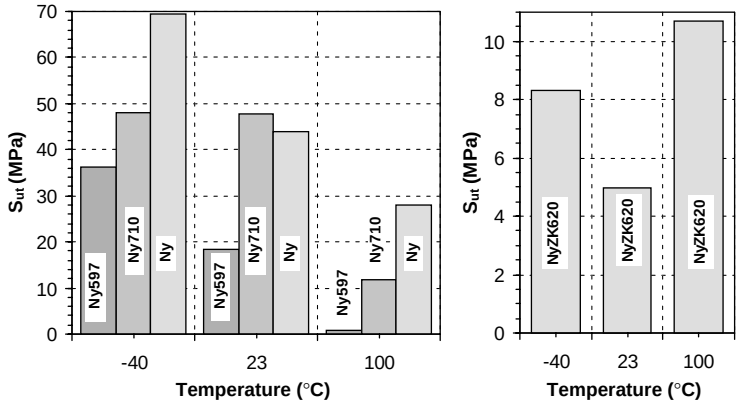

Fig. 5. Tensile strength of three Nylon-based injection molded samples and pure Nylon at three testing temperatures.

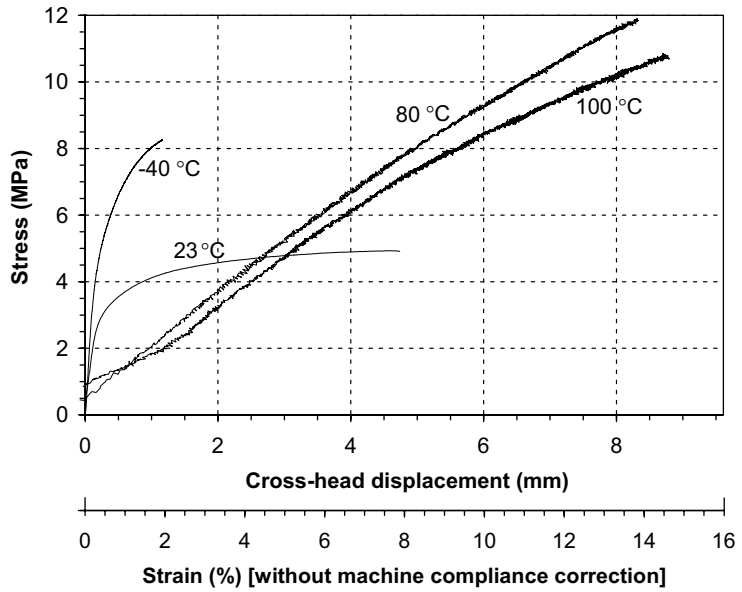

Fig. 6. Tensile stress–strain curves of NyZK620 molded magnets with spherical powder.

of the matrix as the polymer chains elongate and transfer load to the crystalline regions. There is also a severe constraint due to the high volume fraction of the Nd–Fe–B powders. Localized strains in ligaments surrounding the powders can be significantly larger than the nominal strain.

At 23°C, the strain-to-fracture for NyZK620 is much larger than that for Ny597 and Ny710, as previously shown in Fig. 4. The former contains spherical powders while the latter contains irregular shaped powders. This difference in strain-to-fracture can better be illustrated by the dimensional elongation in pictures of deformed test samples shown in Fig. 7. Different levels of strain can be seen on Ny597, NyZK620, and Ny tensile specimens tested at 100°C. The Ny597 sample shown in Fig. 7(a) exhibits a small strain-to-fracture. This specimen maintains nearly the same

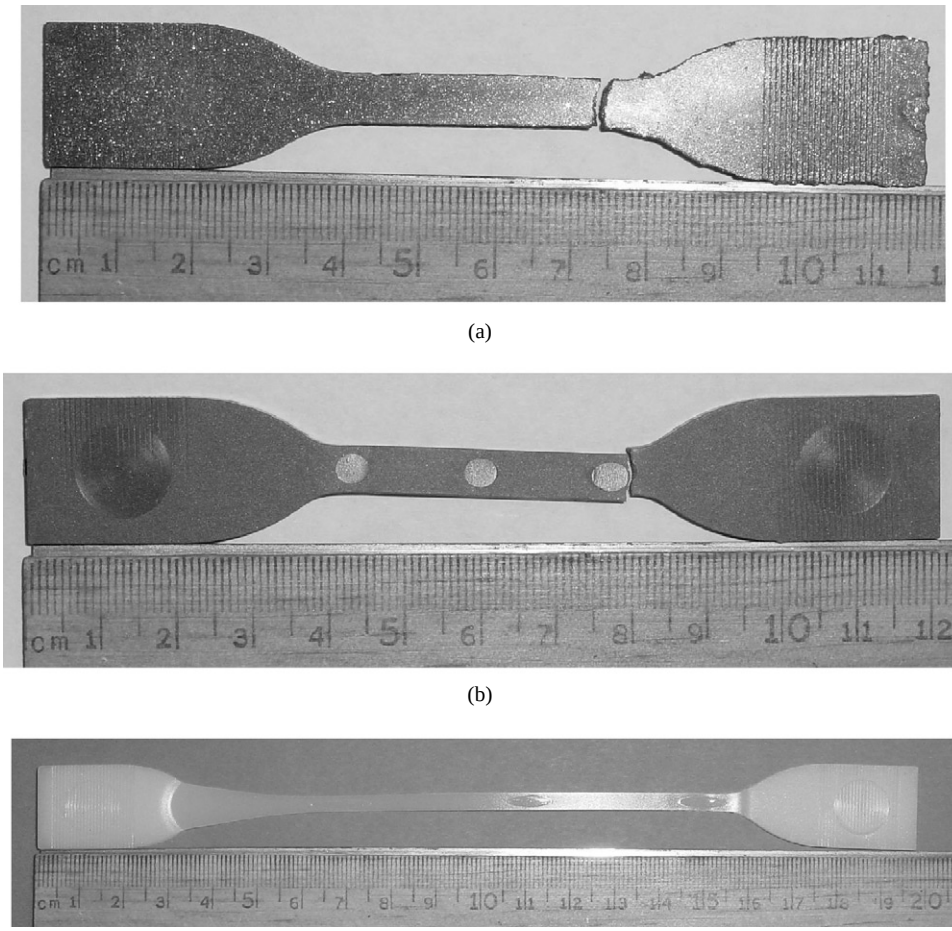

(a)

(b)

(c)

Fig. 7. Pictures of three fractured or deformed tensile test specimens tested at 23°C (a) Ny597, (b) NyZK620, and (c) Ny.

original dimensions. Fig. 7(b) illustrates a relatively large deformation (15% strain) obtained on the NyZK620 specimen at 100°C. For Ny, as shown in Fig. 7(c), the sample continued to deform and did not fracture at the end of the test when 160% strain was reached.

Comparing Ny597 and NyZK620, the volume fraction of magnetic powder for these two specimens differs by merely 2.3 vol%. However, their stain-to-fracture values differ by approximately 20 folds (0.39% and 7.9% for Ny597 and NyZK620, respectively, at 23°C). The low strain-to-fracture of Ny597 may be ascribed to the Nd–Fe–B powders of irregular shapes. The sharp angular powders and perhaps also the fine dispersion of very small angular powders evidently initiate very rapid fracture of the matrix ligaments as strain is increased. The powder angularity causes much larger stress intensification compared to the spherical powders. In addition, the higher stress levels reached for the specimens with irregular shape powders at a given strain will accelerate failure.

The difference in the thermal expansion coefficient of Nylon-11 and Nd–Fe–B may contribute to higher tensile strength at -40°C. The thermal expansion coefficient is about $4–8 \times 10^{-6}/$°C for Nd–Fe–B [17] and $2.3–11 \times 10^{-5}/$°C for Nylon

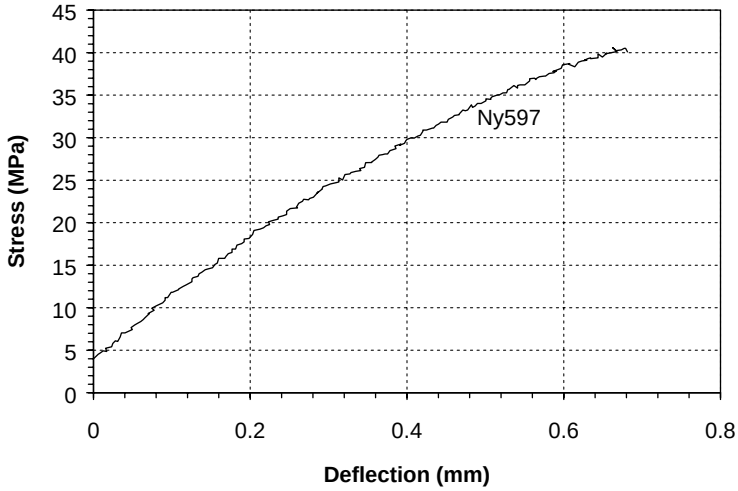

Fig. 8. Flexural four-point-bending test result of Ny597.

[15]. Cooling samples to cryogenic temperature creates a compressive stress at the interface between the Nd–Fe–B powder and Nylon matrix and improves the tensile strength.

3.2. Bending test results

Fig. 8 shows the stress-deflection curve for the bending test of Ny597 at 23°C. The deflection is associated with the measured displacement of loading pins in the four-point bending test configuration. The measured force is used to calculate the maximum bending stress according to

$$\sigma_{\max} = \frac{3PL}{2bd^2}, \tag{1}$$

where P is the load, L (= 38.1 mm) is the difference in span of the supporting and loading rollers, b (= 12.7 mm) is the specimen width of contact with rollers, and d (= 6.4 mm) is the specimen thickness. Seven bending tests were performed and the values represent the arithmetic average of all the measurements. The bending strength of the Ny597 sample is 41 MPa. This strength is higher than the tensile strength of 18 MPa. Such a trend is commonly observed and may be ascribed to the non-uniform distribution of stresses during bending and the difference in volume of material subjected to tensile stresses.

3.3. Young's modulus

Young's modulus can be determined using either the dynamic impulse test as described in ASTM Standard C1259-98 [13] or the tensile test. The dynamic Young's modulus was calculated through the formula given in the ASTM standard [13]

$$E = 0.9465\left(\frac{mf_f^2}{b}\right)\left(\frac{L^3}{t^3}\right)T_1, \tag{2}$$

where E is the Young's modulus, m is the mass of bar in g, b is the width of bar in mm, L is the length of bar in mm, t is the thickness of bar in mm, $f_f (= 2,000,000/R)$ is the fundamental frequency of the bar in flexure in Hz, R is the reading from Grindo-Sonic testing machine, and T_1 is the correction factor as to be determined according to the ASTM Standard [13].

Using values for the Poisson's ratios of 0.2, 0.3 and 0.4, the dynamic Young's moduli for Ny597 determined by the ultrasonic dynamic impulse are 15.69, 15.70, and 15.72 GPa. Young's modulus of the same specimen group calculated from tensile test is 12.7 GPa. The variations in Poisson's ratios of range studied shows limited impact to the dynamic Young's modulus. There is, however, a notable discrepancy (about 20%) between the values determined from the two methods. This differs significantly from that of PPS bonded

Nd–Fe–B magnets of similar shape and size [10,14], where a 5% difference in Young's modulus was obtained. It is likely that Nylon based specimens exhibit larger anisotropy than the PPS counterparts and, therefore, does not render itself for an accurate Young's modulus determination using the dynamic impulse method.

4. SEM micrographs of fractured surfaces

The fractured surfaces were examined using SEM to gain insights of the failure mechanism. Figs. 9(a)–(f) show the fracture surfaces of Ny597 after tensile tests at −40°C, 23°C, and 100°C. The irregularly shaped Nd–Fe–B powders can be

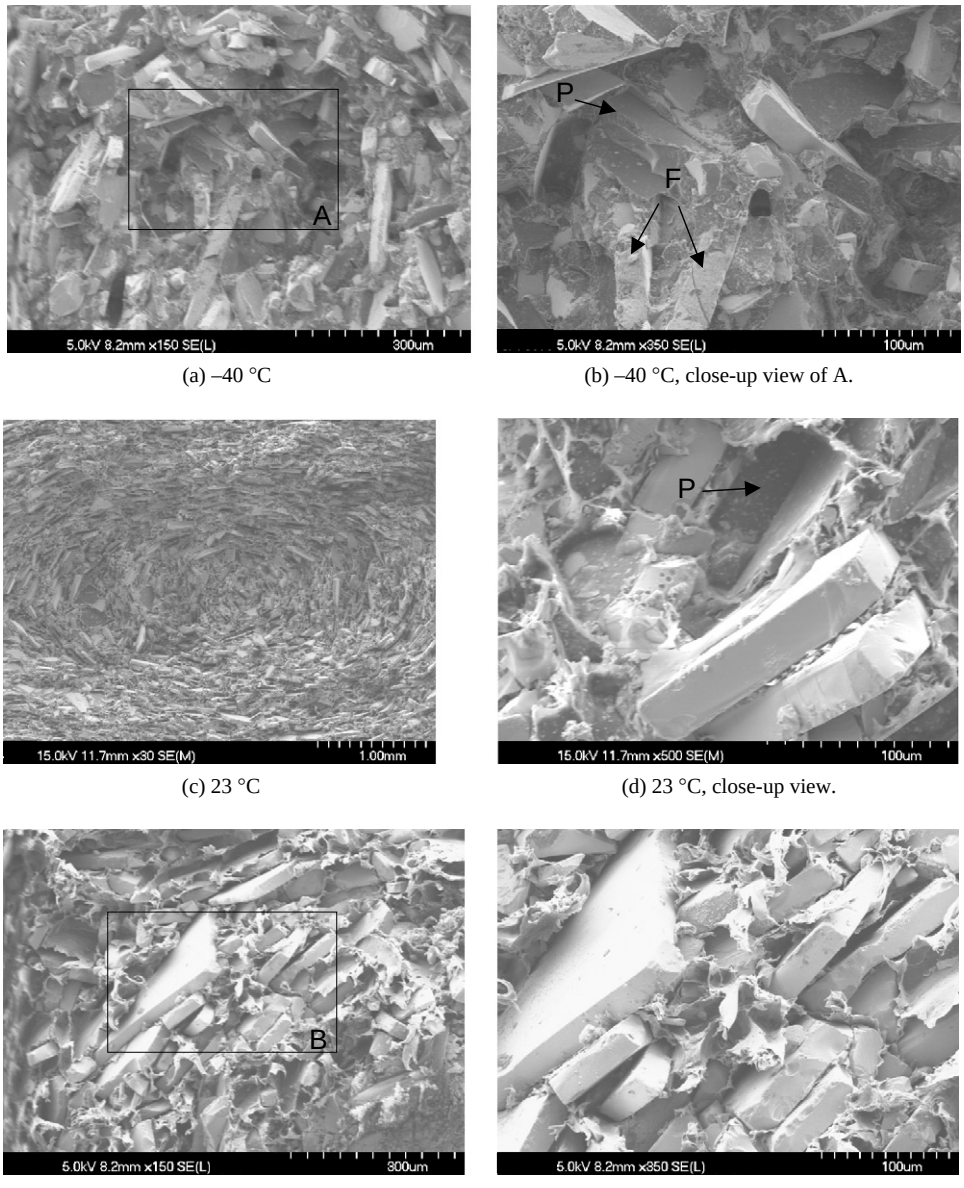

(a) –40 °C (b) –40 °C, close-up view of A.

(c) 23 °C (d) 23 °C, close-up view.

(e) 100 °C (f) 100 °C, close-up view of B.

Fig. 9. SEM micrographs of fracture surfaces of Ny597 with irregular plate shape Nd–Fe–B powder.

observed at the fracture surfaces. It should be noted that the irregularly shaped powders are aligned in the visible pattern as the molten compound flows through the mold during the injection molding process. Such alignment creates a large surface area to resist the sliding between the irregularly shaped Nd–Fe–B powders and the Nylon matrix. This could partially explain the higher tensile strength of specimens prepared from melt spun powders as previously shown in Fig. 5. Such phenomenon was not observed for specimens prepared with spherically shaped atomized powders.

Fig. 9(c) shows an overall view of the fracture surface of a specimen tested at 23°C. A vortex

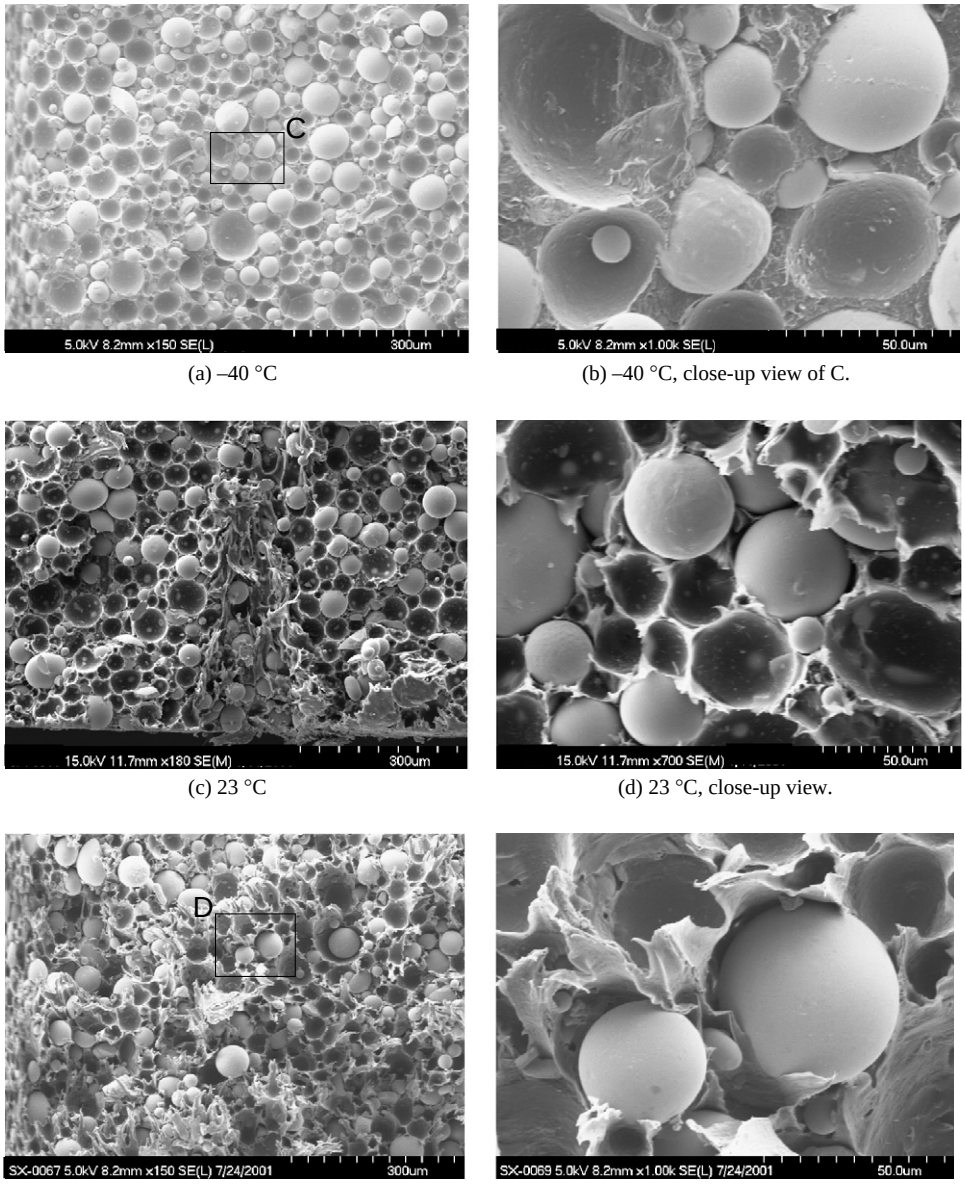

(a) –40 °C (b) –40 °C, close-up view of C.

(c) 23 °C (d) 23 °C, close-up view.

(e) 100 °C (f) 100 °C, close-up view of D.

Fig. 10. SEM micrographs of fracture surfaces of NyZK620 with spherical shape Nd–Fe–B powder.

shaped core can be seen near the center of sample fracture surface. This vortex arises from the fact that the molten compound still flows through the mold as it partly solidifies on the surface during the injection molding process. The solidification starts from the mold surfaces and ends near the center of the vortex. The alignment of irregularly shaped powders along the flow direction helps to retain the brittle characteristics of Nd–Fe–B powders in tensile and bending tests, as previously compared in Figs. 4 and 5. At 23°C, the melt spun Nd–Fe–B powders do not fracture. Instead, they are pulled out and leave pockets on the fracture surface, as marked by P in Fig. 9(d). Figs. 9(e) and (f) show such powder pulled out or debonded from the fracture surface of a specimen tested at 100°C. As Nylon is softened at 100°C, and ligaments of Nylon pulled between magnetic particles on the fracture surface can be recognized. At −40°C, as shown in Figs. 9(a) and (b), the Nylon compound is brittle and the fracture surface is glassy. The fracture of Nd–Fe–B particles, marked by F in Fig. 9(b), can be seen. Some shallow pockets due to particle pull-out can still be identified on the same fracture surface in Fig. 9(b).

Figs. 10(a)–(f) show the fracture surfaces of NyZK620 at −40°C, 23°C, and 100°C. Spherical Nd–Fe–B powders of different size can be identified. Debonding or separation of spherical powders with Nylon matrix may be the dominant failure mechanism as well. At 62.0% volume fraction, the spherical Nd–Fe–B powders are nearly closely packed and provide weak structural supports to the overall composites. Thus, it makes this type of sample very weak under tensile loading when compared to counter samples containing melt spun powders with irregular plate shape. The latter can produce geometric locking and provide better load transfer during straining. The transitions of Nylon from a glassy, brittle fracture surface at −40°C to the morphology with ligaments of Nylon pulled between powders can also be seen in Figs. 10(e) and (f) on the fracture surface of a specimen tested at 100°C.

5. Conclusions

Tensile and bending strength as well as Young's modulus of Nylon bonded Nd–Fe–B magnets have been examined from −40°C to 100°C using specimens prepared from melt spun and atomized powders. It was found that the tensile strength varies significantly with both test temperature and morphology of Nd–Fe–B powder. For a fixed volume fraction of magnetic powder, the tensile strength decreases with increasing temperature. For bonded magnets made of melt spun powder, the tensile strength increases with increasing volume fraction of magnetic powder. Specimens made of spherical atomized powders exhibit much lower tensile strengths when compared to those made of melt spun powder. SEM analysis indicated that the debonding of Nd–Fe–B powder and Nylon interface is the main cause of failure at 23°C and 100°C. Fracture of Nd–Fe–B particles was observed on magnets prepared from melt spun powders at −40°C and contributed to a different failure mechanism. This research also identified the excellent flexibility of bonded magnets with spherical shape Nd–Fe–B powder.

Acknowledgements

Portion of this research was sponsored by the Assistant Secretary for Energy Efficiency and Renewable Energy, Office of Transportation Technologies, as part of the High Temperature Materials Laboratory User Program, Oak Ridge National Laboratory, managed by UT-Battelle, LLC for the US Department of Energy under contract number DE-AC05-00OR22725 and by National Science Foundation Grant #9983582 (Dr. K.P. Rajurkar, Program Director). The authors also gratefully acknowledge the help of Chris Stevens, Ken Liu, and Dorothy Coffey at the High Temperature Materials Laboratory of Oak Ridge National Laboratory.

References

[1] J.J. Croat, J.F. Herbst, R.W. Lee, F.E. Pinkerton, J. Appl. Phys. 55 (1984) 2078.
[2] M. Sagawa, S. Fujimura, N. Togawa, H. Yamamoto, Y. Matsuura, J. Appl. Phys. 55 (1984) 2083.
[3] J.M.D. Coey (Ed.), Rare-Earth Iron Permanent Magnets, Oxford University Press, Oxford, 1996.

[4] B.M. Ma, J.W. Herchenroeder, B. Smith, M. Suda, D.N. Brown, Z. Chen, J. Magn. Magn. Mater. 239 (2002) 418.
[5] J. Jiang, Z. Zeng, J. Wu, M. Tokunaga, J. Magn. Magn. Mater. 214 (2000) 61.
[6] J.A. Horton, J.L. Wright, J.W. Herchenroeder, IEEE Trans. Magn. 32 (1996) 4374.
[7] Y.M. Rabinovich, V.V. Sergeev, A.D. Maystrenko, V. Kulakovsky, S. Szymura, H. Bala, Intermetallics 4 (1996) 641.
[8] K. Ikuma, K. Akioka, T. Shimoda, R. Watanabe, H. Miyadera, IEEE Trans. J. Magn. Jpn. 9 (1994) 94.
[9] J. Xiao, J.U. Otaigbe, Polym. Composites 21 (2000) 332.
[10] M.G. Garrell, B.M. Ma, E. Lara-Curzio, A.J. Shih, R.O. Scattergood, Mechanical properties of PPS injection molded Nd–Fe–B permanent magnets, Intermag Europe 2002, April 28–May 2, Amsterdam, Netherlands.
[11] ASTM standard D638-99, Standard Test Method for Tensile Strength of Plastics, American Society for Testing and Materials, Pennsylvania, 1999.
[12] ASTM standard D790-99, Standard Test Methods for Flexural Properties of Unreinforced and Reinforced Plastics and Electrical Insulation Materials, American Society for Testing and Materials, Pennsylvania, 1999.
[13] ASTM standard C1259-98, Standard Test Method for Dynamic Young's Modulus, Shear Modulus, and Poisson's Ratio for Advanced Ceramics by Impulse Excitation of Vibration, American Society for Testing and Materials, Pennsylvania, 1998.
[14] M.G. Garrell, Mechanical properties of injection molded permanent magnets, MS Thesis, NC State University, 2002.
[15] N.A. Waterman, M.F. Ashby, The Materials Selector, Vol. 1, 2nd Edition, Chapman & Hall, New York, 1997.
[16] W.D. Callister, Materials Science and Engineering, Wiley, New York, 1985, p. 357.
[17] C.H. Chen, M.S. Walmer, M.H. Walmer, W. Gong, B.M. Ma, J. Appl. Phys. 85 (8) (1999) 5669.